

CONTRIBUTION FROM THE PAUL M. GROSS CHEMICAL LABORATORY,  
DUKE UNIVERSITY, DURHAM, NORTH CAROLINA 27706

## Polarized Crystal Spectra of Bis(DL-histidinato)nickel(II) Monohydrate and Bis(L-histidinato)nickel(II) Monohydrate<sup>1</sup>

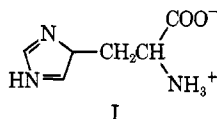
BY P. L. MEREDITH AND R. A. PALMER\*

Received August 10, 1970

The polarized single-crystal electronic spectra of Ni(DL-his)<sub>2</sub>·H<sub>2</sub>O (specifically the racemic lattice compound Ni(D-his)<sub>2</sub>Ni(L-his)<sub>2</sub>·2H<sub>2</sub>O) and of Ni(L-his)<sub>2</sub>·H<sub>2</sub>O have been obtained at ambient and cryogenic temperatures (his = histidine). For the orthorhombic crystal of the racemate, the molecular polarizations have been calculated from the spectra measured with the electric vector of the radiation parallel to the crystallographic axes. The correction for the 11° misalignment of the molecular axes with respect to the extinction directions is seen to be minimal. The spectra of the monoclinic levo crystal show only moderate intensity variations from those of the racemic crystal. Comparison of the crystal spectra to that of the aqueous solution supports the assumption of the oriented gas model. Using the spectra of the racemic crystal as a guide, the molecular spectra have been interpreted in terms of the triaxial point group C<sub>2v</sub>. Intensity not conforming to the pure electric dipole selection rules has been shown to be very temperature dependent. Allowing vibrations have been assigned for these vibronic transitions. The observed maxima have been compared by least-squares analysis to the eigenvalues calculated in a ligand field model in which the potential is expanded in terms of tesseral harmonics. Fitting the spectra as assigned using the C<sub>2v</sub> selection rules gives a Dq of -1125 cm<sup>-1</sup> while B and C are found to be 783 and 3653 cm<sup>-1</sup>, respectively. In the analysis nine experimentally observed bands have been fit to ±100 cm<sup>-1</sup>.

### Introduction

The structure of transition metal complexes of amino acids has received much attention in recent years due to the possible role of these complexes as models for the more complicated enzymatic systems activated by metal ions. One of the most frequently encountered amino acids in these processes is histidine (I). Since



free histidine has three basic sites of widely differing pK<sub>a</sub>'s, the nature of its interactions with metal ions is strongly pH dependent. It is one of the strongest metal coordinators among the amino acids<sup>2</sup> and it plays an important role in the binding of metals by proteins, principally, if not entirely, through its imidazole function. In simple complexes with metal ions histidine has been observed both as a bidentate and as a tridentate chelating ligand.

There are in the literature numerous studies dealing with histidinate complexes in solution.<sup>3-22</sup> On the

other hand, there are relatively few papers describing the isolation and characterization of individual metal-histidine complexes in the solid state. Isolation of complexes of platinum(II),<sup>23-25</sup> molybdenum(V),<sup>26</sup> and cobalt(III)<sup>27</sup> have been described. In addition, isolation of the oxygenated compound [Co(L-his)<sub>2</sub>]<sub>2</sub>O<sub>2</sub> has been reported,<sup>28</sup> though its structure is still unknown. The structures of two zinc(II)-histidine complexes have been determined,<sup>29-30</sup> as well as structures of bis(DL-histidinato)nickel(II),<sup>31</sup> bis(L-histidinato)cobalt(II),<sup>32,33</sup> D-histidinato-L-histidinato-cobalt(II),<sup>34</sup> bis(L-histidine)copper(II) dinitrate dihydrate,<sup>35</sup> and bis(L-histidinato)cadmium(II).<sup>32</sup>

In this paper we report our polarized spectral results for single crystals of Ni(DL-his)<sub>2</sub>·H<sub>2</sub>O and Ni(L-his)<sub>2</sub>·H<sub>2</sub>O (his = histidine).<sup>36</sup> In both compounds, the histidinate ion acts as a tridentate ligand, coordinating to the metal atom through three of the four possible functional groups. These are (a) the carboxyl group (or oxygen), O, (b) the α-amino group, N<sub>A</sub>, and (c) the imidazole nitrogen next to the alanine residue, N<sub>I</sub>.

(1) (a) Presented in part at the 155th National Meeting of the American Chemical Society, San Francisco, Calif., 1968; see Abstract M 124; (b) taken in part from the Ph.D. thesis of P. L. Meredith, Duke University, 1970.

(2) A. Albert, *Biochem. J.*, **47**, 531 (1950); **50**, 690 (1952).

(3) R. H. Carlson and T. L. Brown, *Inorg. Chem.*, **5**, 26 (1966), and references cited therein.

(4) D. D. Ferrin and V. S. Sharma, *J. Chem. Soc. A*, 724 (1967).

(5) O. N. Puplikova, L. N. Akimova, and I. A. Savich, *Vestn. Mosk. Univ., Khim.*, **21**, 106 (1966).

(6) A. C. Andrews, and D. M. Zebolsky, *J. Chem. Soc.*, 742 (1965).

(7) E. V. Raju and H. B. Mathur, *J. Inorg. Nucl. Chem.*, **31**, 425 (1969), and references cited therein.

(8) J. H. Ritsma, J. C. Van De Grampel, and F. Jellinek, *Recl. Trav. Chim. Pays-Bas*, **88**, 411 (1969).

(9) W. F. Stack and H. A. Skinner, *Trans. Faraday Soc.*, **63**, 1136 (1967).

(10) O. N. Puplikova, L. N. Akimova, and I. A. Savich, *Vestn. Mosk. Univ., Khim.*, **21**, 56 (1966).

(11) O. N. Puplikova and U. A. Savich, *ibid.*, **24**, 80 (1969).

(12) C. C. MacDonald and W. D. Phillips, *J. Amer. Chem. Soc.*, **85**, 3736 (1963).

(13) R. B. Martin and R. Mathur, *ibid.*, **87**, 1065 (1965).

(14) K. M. Wellman and B. K. Wong, *Proc. Nat. Acad. Sci. U. S.*, **64**, 824 (1969).

(15) B. Sarkar and Y. Wigfield, *J. Biol. Chem.*, **242**, 5572 (1967).

(16) E. W. Wilson, Jr., and R. B. Martin, *Inorg. Chem.*, **9**, 528 (1970).

(17) D. W. Urry and H. Eyring, *J. Amer. Chem. Soc.*, **86**, 4574 (1964).

(18) D. Kivelson and R. Neiman, *J. Chem. Phys.*, **35**, 149 (1961).

(19) R. W. Hay and P. J. Morris, *Chem. Commun.*, 18 (1969).

(20) J. Simplicio and R. G. Wilkins, *J. Amer. Chem. Soc.*, **89**, 6092 (1967).

(21) M. A. Doran, S. Chaberek, and A. E. Martell, *ibid.*, **86**, 2129 (1964).

(22) V. S. Sharma, J. Schubert, H. B. Brooks, and F. Sicilio, *ibid.*, **92**, 822 (1970).

(23) L. M. Volshstein and I. C. Luk'yanova, *Russ. J. Inorg. Chem.*, **11**, 708 (1966).

(24) L. M. Volshstein and L. D. Dikanskaya, *ibid.*, **13**, 1304 (1968).

(25) V. Balice and T. Theophanides, *J. Inorg. Nucl. Chem.*, **32**, 1237 (1970).

(26) L. R. Melby, *Inorg. Chem.*, **8**, 1539 (1969).

(27) L. J. Zompa, *Chem. Commun.*, 783 (1969).

(28) Y. Sano and H. Tanabe, *J. Inorg. Nucl. Chem.*, **25**, 11 (1963).

(29) R. H. Kretsinger, F. A. Cotton, and R. F. Bryan, *Acta Crystallogr.*, **18**, 651 (1963).

(30) M. M. Harding and S. J. Cole, *ibid.*, **16**, 643 (1963).

(31) K. A. Fraser and M. M. Harding, *J. Chem. Soc. A*, 415 (1967).

(32) K. A. Fraser and M. M. Harding, *Chem. Commun.*, 344 (1965).

(33) M. M. Harding and H. A. Long, *J. Chem. Soc. A*, 2554 (1968).

(34) R. Candlin and M. M. Harding, *ibid.*, **A**, 384 (1970).

(35) B. Evertsson, *Acta Crystallogr., Sect. B*, **25**, 30 (1969).

(36) The -ate nomenclature is appropriate since it reflects the fact that these complexes are formally carboxylate salts. As stated in the abstract the racemic crystal is specifically the lattice compound Ni(D-his)<sub>2</sub>Ni(L-his)<sub>2</sub>·H<sub>2</sub>O. For brevity we will here refer to it as either Ni(DL-his)<sub>2</sub>·H<sub>2</sub>O or bis(DL-histidinato)nickel(II) monohydrate.

CRYSTAL HABIT and MOLECULAR  
PACKING in  
 $\text{Ni}(\text{D,L-HISTIDINATE})_2 \cdot \text{H}_2\text{O}$

A - NORMAL HABIT  
B -  $b$  VIEW (010)  
C -  $c$  VIEW (001)

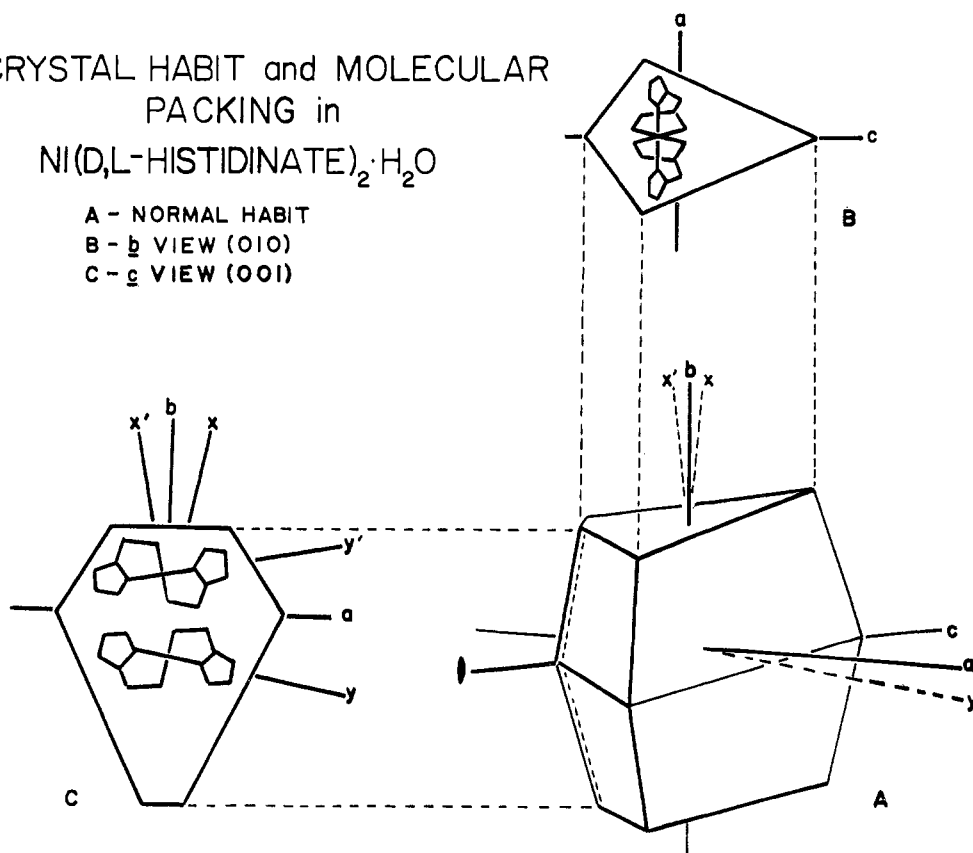


Figure 1.—Crystal morphology of  $\text{Ni}(\text{DL-his})_2 \cdot \text{H}_2\text{O}$ .

### Experimental Section

**Source of Reagents.**—L-Histidine and DL-histidine were obtained from Nutritional Biochemicals Corp., Cleveland, Ohio, and nickel(II) carbonate was from Baker and Adamson Products, Morristown, N. J. Reagents were used without further purification.

**Growth of Single Crystals.**—All crystals were grown from aqueous solution. For example, 2.04 g of DL-histidine was dissolved in 20 ml of warm water and 0.809 g of  $\text{NiCO}_3$  was added. This mixture was heated until evolution of  $\text{CO}_2$  ceased and all the  $\text{NiCO}_3$  had reacted. A deep blue-purple solution (pH 7.2) resulted. From the filtered solution large, well-formed blue-purple crystals appeared within a few hours. These crystals have a percentage of carbon, hydrogen, and nitrogen corresponding to the formula  $\text{Ni}(\text{his})_2 \cdot 2\text{H}_2\text{O}$ . Along with the blue-purple crystals of the dihydrate appeared a "background" of pink-purple crystals of recognizable regular habit but too small to be used conveniently for spectral purposes. These small crystals were induced to grow larger by raising the pH of the solution with NaOH to between 10 and 11. At this pH the pink-purple crystals dominated and relatively large specimens, several millimeters on a side, could be obtained by slow evaporation. The crystals were verified to be  $\text{Ni}(\text{DL-his})_2 \cdot \text{H}_2\text{O}$  by X-ray diffraction determination of the space group<sup>31</sup> and by C, H, and N analyses by Galbraith Laboratories, Inc., Knoxville, Tenn.

**Instrumentation.**—All spectra were measured with a Cary Model 14R recording spectrophotometer using the visible and IR-1 modes. A high-intensity tungsten halide source, pen period control, and near S-20 photomultiplier tube were used to enhance the quality of the spectra. The light was polarized by a calcite ultraviolet DC-200 Glan-Thompson prism (Crystal Optics, Chicago, Ill.) placed in the entrance window of the sample compartment. An iris diaphragm and/or neutral density filters were used to attenuate the reference beam. For spectra obtained at liquid nitrogen temperatures a fused-quartz cryostat (H. S. Martin and Co., Model M203908-S (modified)) was used. For spectra at helium temperatures an Andonian Associates Model 0-24/7M variable-temperature cryostat was used. The sample temperature in the Andonian cryostat was measured by a calibrated germanium resistor and a conductance bridge. The

temperature was between 4 and 5°K throughout the measurement of all spectra nominally classified below as "5°K."

The crystals were mounted over appropriately sized holes in brass plates and masked to prevent light leaks and reflection with Apiezon Q putty. The alignment of the crystals was verified with the aid of a polarizing microscope using extinction directions and interference figures correlated with the orientation of the crystal axes as determined by Weissenberg photographs. The mounting plates were then attached to a room-temperature or cryostat mount and the crystals were positioned at the focus of the Cary 14R sample beam.

Solution spectra were measured by standard techniques in 1-cm Pyrex cells in the Cary 14R.

**Analysis of Spectral Data.**—A base line, determined by measuring the polarized spectrum of an empty mounting plate (with the same size hole as used for the crystal) positioned in the cryostat, was subtracted from each spectrum. This was necessary since an isomorphous, colorless crystal does not exist.

The band envelopes of overlapping bands were approximated by drawing in curves (1) so that at any value of  $\nu$  the sum of the analyzed parts equaled the total absorbance and (2) so that the bands approximated the normal symmetric shape of an isolated absorption band.

Absolute and relative strengths of the transitions giving rise to the spectral bands were determined in terms of integrated band intensities,  $I$ , where  $I = \int (\epsilon/\nu) d\nu$  which for reasonably symmetric bands can be approximated as  $I \approx (1/\nu_{\text{max}}) \int \epsilon d\nu$ . The molar absorptivity,  $\epsilon$ , has the usual significance, *i.e.*,  $A = \epsilon cl$ , where absorbance,  $A = -\log I/\log I_0$ , concentration,  $c$ , is in units of moles per liter of crystal or solution, and path length,  $l$ , is in units of centimeters. Note that  $I$  is in units of molar absorptivity. The molar concentration of the crystals was determined using the formula  $c = 10^3 d/M$  where  $d$  is the density of the crystal (determined and/or verified in this instance by flotation in chloroform-bromoform mixtures) and  $M$  is the molecular weight.

For vibronic bands the expression  $I_T = I_0 \coth(h\theta/2kT)$ <sup>37</sup> was used to approximate  $\theta$ , the electronic ground-state frequency of

(37) O. G. Holmes and D. S. McClure, *J. Chem. Phys.*, **26**, 1686 (1957).

the intensity-producing normal mode. The integrated band intensity at 5°K was assumed equal to  $I_0$  in the above expression.

The areas of the spectral bands were measured by planimeter with accuracy  $\pm 0.1 \text{ cm}^2$ . The scale of the spectra, replotted after conversion of Ångström units to wave numbers ( $\text{cm}^{-1}$ ), was such that the areas ranged between 10 and 50  $\text{cm}^2$  for most bands. Thus, the error in area measurement should be small compared to other experimental uncertainties.

Calculations were performed using the IBM 360/75 computer at Triangle Universities Computer Center (TUCC), Research Triangle Park, N. C.

### Crystal Structure and Morphology

$\text{Ni}(\text{DL-his})_2 \cdot \text{H}_2\text{O}$ .<sup>36</sup>—The crystal structure of  $\text{Ni}(\text{DL-his})_2 \cdot \text{H}_2\text{O}$  has been determined by Fraser and Harding.<sup>31</sup> The deep purple crystal is orthorhombic with space group  $Aba2$ ,  $a = 15.18$ ,  $b = 13.05$ ,  $c = 7.72 \text{ \AA}$ , and  $Z = 4$ . The normal habit of the crystal is illustrated in Figure 1. Spectra were measured with light incident normal to the (001) zone ("c view") and the (010) zone ("b view") of the crystal. In each case, sections of suitable thickness were ground and polished with their faces normal to the appropriate crystallographic axis. The thickness of the plates was measured with a microscope ocular which was calibrated with an objective micrometer slide. The measurements are believed to give the thickness within  $\pm 5\%$ . The "b view" was relatively easy to obtain since the (010) face is prominent in the normal habit. These faces could be perfected by allowing polished crystals to stand in a saturated solution for a few hours. The (001) faces do not develop naturally; thus, crystal plates for the "c view" could be obtained only by mechanical polishing and were not as high in optical quality as the naturally polished "b view".

The crystals contain equal numbers of  $\text{Ni}(\text{D-his})_2$  and  $\text{Ni}(\text{L-his})_2$  molecules related by  $b$ -glide planes. The site symmetry of the nickel atoms is  $C_2$ . The orientation of the molecules within the unit cell and with respect to the crystallographic axes is shown in Figure 1. The  $C_2$  axes of the molecules (the  $z$  molecular axes) are parallel to the twofold screw axes and to the  $c$  crystallographic axis. The  $x$  molecular axis bisects the  $\text{N}_A\text{-Ni-O}$  angles (which have been shown to be only  $80^\circ$ <sup>31</sup>) and the  $y$  molecular axis is approximately along the  $\text{Ni-N}_I$  bonds. (These deviate from collinearity by  $2.4^\circ$ .) The  $x$  and  $y$  molecular axes have two different orientations  $11.3^\circ$  to either side of the crystallographic  $b$  and  $a$  axes, respectively, in the  $ab$  plane.

$\text{Ni}(\text{L-his})_2 \cdot \text{H}_2\text{O}$ .—The structure of  $\text{Ni}(\text{L-his})_2 \cdot \text{H}_2\text{O}$  is reported<sup>38</sup> to be isomorphous with that of  $\text{Co}(\text{L-his})_2 \cdot \text{H}_2\text{O}$ ,<sup>38</sup> which is monoclinic with space group  $C_2$ ,  $a = 29.44$ ,  $b = 8.324$ ,  $c = 6.347 \text{ \AA}$ ,  $\beta = 90.0^\circ$ , and  $Z = 4$ . The crystals are obtained as rhombic needles elongated along the  $b$  axis with both the  $a$  and  $c$  axes projecting out of the most prominent flat face. (The  $a$  axis makes an angle of  $24^\circ$  with this face.) Thus, in the two crystal views obtained, spectra could be measured with light  $\parallel b$  in both cases. The other polarizations were  $\parallel c$  and approximately  $\parallel a$ . Assuming the molecular axes to be assigned in the same manner as in  $\text{Ni}(\text{DL-his})_2 \cdot \text{H}_2\text{O}$ , this implies that spectra can be measured  $\parallel x$  and approximately  $\parallel y$  or  $\parallel z$ .

Although the space group of the  $\text{Ni}(\text{L-his})_2 \cdot \text{H}_2\text{O}$  crystal is different from that of its racemic analog, the molecular packing is essentially the same. Since the axes of

the levo crystal are orthogonal (accidentally), the same views of the molecular array can ostensibly be obtained. However, the orientation of the axes with respect to the faces considerably complicates the experiment and makes conversion from crystal to molecular polarization ratios less certain.

### Results

$\text{Ni}(\text{DL-his})_2 \cdot \text{H}_2\text{O}$ .—The natural or "b view" shows a strongly dichroic scheme:  $\vec{E} \parallel c$ , rose-pink;  $\vec{E} \parallel a$ , deep purple. The "c view" is also strongly dichroic:  $\vec{E} \parallel b$ , pale blue-gray (almost colorless);  $\vec{E} \parallel a$ , deep purple. In both views extinction occurs parallel to the crystallographic axes as required by symmetry. The "b view" and "c view" polarized spectra at 80°K measured along the extinction directions are shown in Figure 2.

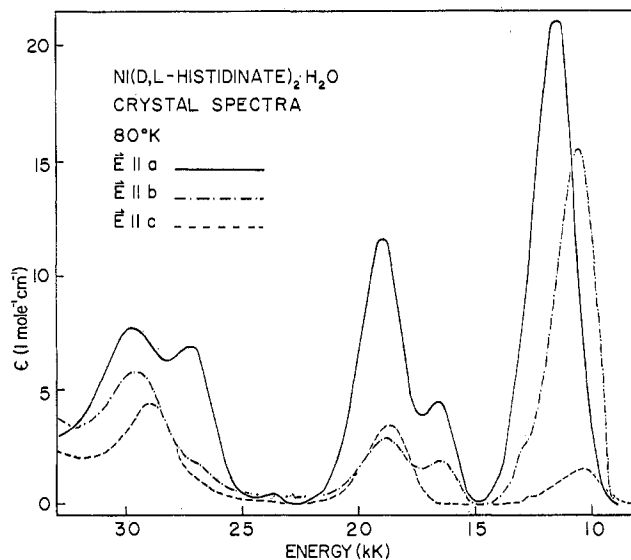


Figure 2.—Polarized spectra of  $\text{Ni}(\text{DL-his})_2 \cdot \text{H}_2\text{O}$  at 80°K.

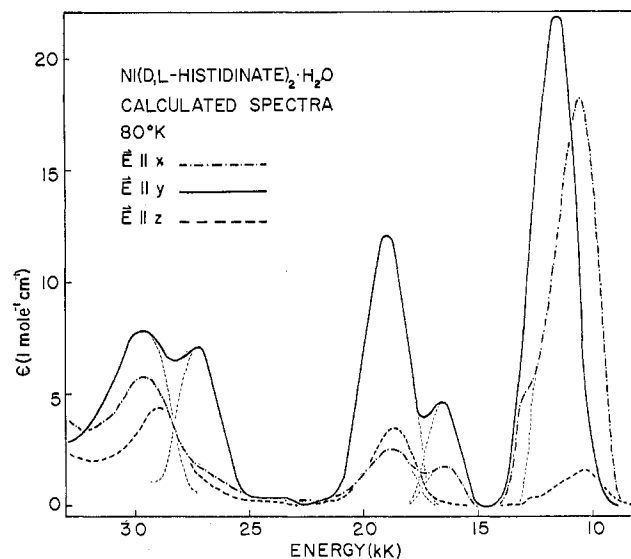


Figure 3.—Calculated molecular spectra along  $x$ ,  $y$ , and  $z$  axes in  $\text{Ni}(\text{DL-his})_2 \cdot \text{H}_2\text{O}$  at 80°K.

Note that the  $a$  polarization is common to both views. From these data the molecular polarizations, that is, the spectra which would be observed with the electric vector of the light along the molecular  $x$ ,  $y$ , and  $z$  axes, have been calculated. The calculated  $x$ ,  $y$ , and  $z$  spectra at 80°K are given in Figure 3. The energies,

(38) M. M. Harding, private communication.

TABLE I  
 SPECTRAL DATA FOR Ni(DL-his)<sub>2</sub>·H<sub>2</sub>O AT 300, 80, AND 5°K

Polarization of electric vector, $\vec{E}$	$\nu_{\max}(5^\circ\text{K})$ , kK	Integrated band intensity, $I$			$\Delta I(300-80^\circ\text{K})$ , %	Molar absorptivity, $\epsilon$			Allowing mode $\theta$ , cm <sup>-1</sup> Symmetry Energy <sup>a</sup>	
		300°	80°	5°		300°	80°	5°		
x	10.6	4.3	4.0	3.7	5	16.4	18.1	16.5	...	...
	16.5	0.26	0.18	0.17	33	2.3	1.8	1.8	$\beta_2$	324
	18.8	0.48	0.32	0.30	32	3.2	2.6	2.6	$\alpha_2$	300
	29.6	0.66	0.39	0.38	40	5.4	3.9	3.8	$\beta_2$	273
	11.4	4.2	4.1	3.8	5	18.4	21.8	20.0	...	...
y	16.5	0.64	0.44	0.43	31	4.7	4.6	4.6	$\beta_1$	340
	19.0	1.6	1.4	1.4	11	11.4	12.0	11.4	...	...
	27.3	0.64	0.50	0.40	21	5.5	5.1	7.5	...	...
	29.6	0.72	0.66	0.53	19	8.4	5.9	5.5	$\beta_1$	390
	10.6	0.72	0.33	0.25	54	2.3	1.6	1.2	$\beta_1$	150
z	18.9	0.48	0.42	0.45	10	3.6	3.5	4.4	...	...
	28.8	0.38	0.35	0.34	6	3.2	3.6	4.0	...	...

<sup>a</sup> As calculated by the approximation of Holmes and McClure;<sup>37</sup> see text.

integrated band intensities, and molar absorptivities of the observed and calculated maxima at 300, 80, and 5°K are given in Table I.

Ni(L-his)<sub>2</sub>·H<sub>2</sub>O.—Microscopic observation again demonstrates distinct dichroism: with  $\vec{E}||b$ , blue-gray (almost colorless); with  $\vec{E}||a$ , deep purple. (Thus, as in the racemic crystal, interaction of the molecule with light seems most significant in the "out-of-plane" direction, *i.e.*, along the N<sub>I</sub>-Ni-N<sub>I</sub> direction). Extinction directions are parallel and perpendicular to the needle axis. The energies and molar absorptivities of the observed maxima are given in Table II.

 TABLE II  
 SPECTRAL DATA FOR Ni(L-his)<sub>2</sub>·H<sub>2</sub>O

Polarization of electric vector, $\vec{E}$	$\nu_{\max}(80^\circ\text{K})$ , kK	Molar absorptivity, $\epsilon$	Polarization of electric vector, $\vec{E}$	$\nu_{\max}(80^\circ\text{K})$ , kK	Molar absorptivity, $\epsilon$
x	10.5	20	y	23.9	0.9
	16.5	1.4		27.1	19
	18.8	2.4		29.2	13
	29.5	4.9		z	10.8
y	11.5	8.8	16.3 sh		0.7
	16.4	6.4	18.8		4.0
	18.7	21	27.0 sh		1.5
	23.4	1.0	29.0		3.6

In both crystals the three-band systems observed are as expected for a nickel(II) atom in an effective ligand field of approximately octahedral symmetry. The similarities between the spectra of the DL case and the L case, while not exact, are quite close. The obvious splitting of and energy separation of the band maxima suggest that the same intensity-gaining mechanism is effective in both crystals. The *x* spectra in the two systems correspond almost exactly. A very intense band occurs at 10.5 kK, two maxima occur at 16.5 and 18.8 kK in the visible region, and one band occurs at 29.4 kK in the near-uv region. The *y* and *z* spectra do not correspond quite as closely with respect to intensities but five distinct bands of about the same energy are apparent in each case. Spin-forbidden bands appear to be more prominent in the levo case. Particularly striking are the weak, but well-defined bands between 23.0 and 24.0 kK. The similarities described here imply that the absorption is due chiefly to molecular properties and that crystal-packing interactions are negligible in their effect on the energies of the electronic spectra in these cases.

**Nickel(II)-DL-Histidine Solution Spectra.**—Previous workers have reported absorption spectra of solutions of nickel(II) and histidine in the visible region.<sup>10</sup> In this paper we report spectra obtained at various pH's in the infrared, visible, and near-ultraviolet regions for comparison to the crystal data. Three broad Gaussian bands occur in the spectrum at 10.7, 18.0, and 28.0 kK. At low pH (3.18) the middle band shows a distinct splitting reminiscent of that seen in solutions containing the Ni(H<sub>2</sub>O)<sub>6</sub><sup>2+</sup> cluster,<sup>39</sup> implying that the amino acid has been completely protonated and that the pale green hexaaquo complex is probably the primary species in solution. As pH increases, the band maxima move to higher energies. This spectral shift is observed visually as the color changes from green to pale blue to purple-blue and finally to deep blue-purple, the color of the Ni(DL-his)<sub>2</sub>·H<sub>2</sub>O crystals. Other than the splitting of the middle band at low pH, there is minimal evidence of broadening or splitting in these solution spectra (Figure 4).

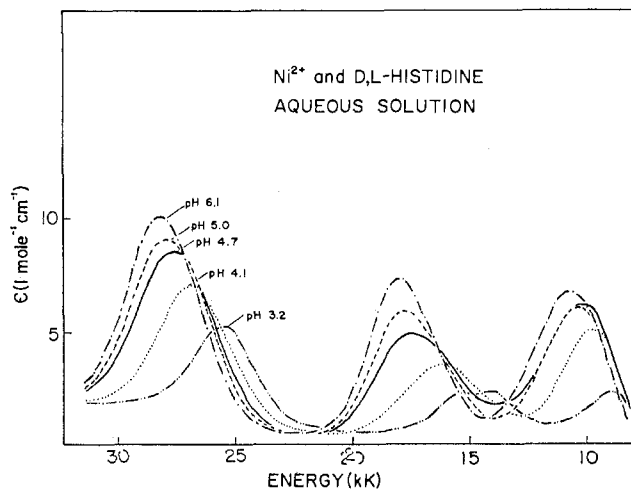


Figure 4.—Solution spectra of Ni<sup>2+</sup> and DL-histidine as a function of pH.

**Calculation of Spectral Ligand Field Parameters.**—In fitting the spectra to a set of crystal field parameters we have used a computer program called "d<sup>2</sup> Spectral Calculation and Hunt" (DTWOSCH), written and generously provided by Couch.<sup>40</sup> The electrostatic poten-

(39) C. K. Jørgensen, *Acta Chem. Scand.*, **10**, 887 (1956).

(40) T. W. Couch, Ph.D. Dissertation, University of Tennessee, 1968.

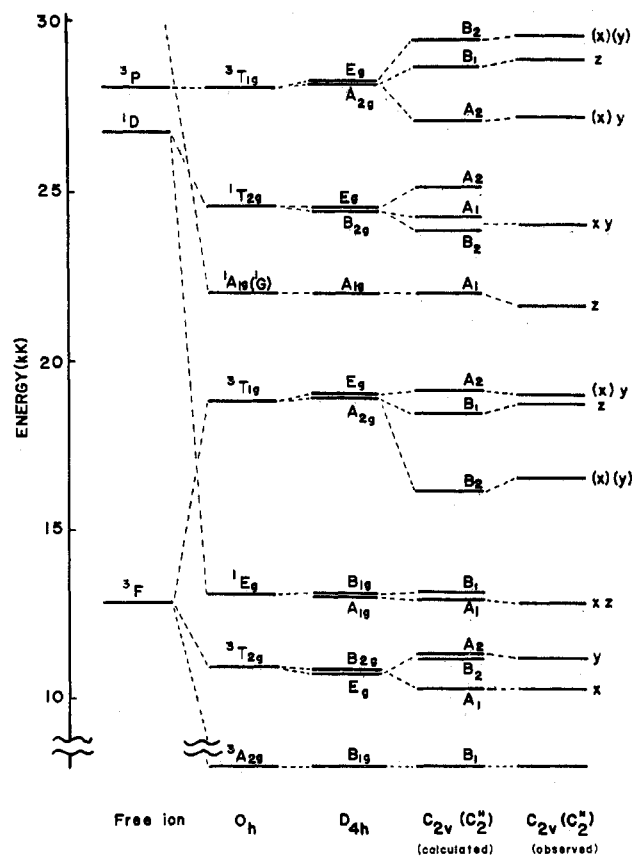


Figure 5.—Calculated and observed energy levels for Ni(DL-his)<sub>2</sub>·H<sub>2</sub>O with free-ion and high-symmetry parentage shown. Electronic polarization is indicated by x, y, or z; vibronic polarization is indicated by (x), (y), or (z).

tial at a point  $(r_i, \theta_i, \phi_i)$  near the metal atom site as origin is expanded over a sum of tesseral harmonics,  $Z_{nm}(\theta_i, \phi_i)$

$$V(r_i, \theta_i, \phi_i) = \sum_{n,m} \gamma_{nm}^c r_i^n Z_{nm}^c(\theta_i, \phi_i)$$

where the coefficients  $\gamma_{nm}^c$  are given by a sum over the ligand charges  $(R_j, \theta_j, \phi_j)$

$$\gamma_{nm}^c = \sum_j \frac{4\pi}{2n+1} q_j \frac{Z_{nm}^c(\theta_j, \phi_j)}{R_j^{n+1}}$$

The method of calculation has been described by Prather<sup>41</sup> and applied to garnets containing the Yb<sup>3+</sup> ion.<sup>42</sup> The program DTWOSCH has been used successfully to fit electronic spectra of nickel(II) chloride complexes in a low-symmetry field.<sup>43</sup>

For  $C_{2v}$  symmetry and suitably chosen axes, only terms with even values of  $n$  and  $m$  will have any effect, and for d electrons, only those with  $n \leq 4$  need be included. Thus, five nonzero values of  $\Gamma_{nm}^c$  must be included:  $\Gamma_{20}$ ,  $\Gamma_{40}$ ,  $\Gamma_{22}$ ,  $\Gamma_{42}$ , and  $\Gamma_{44}$ . The  $\langle d^2; SLJM' | V | d^2; SLJM' \rangle$  matrix elements are then calculated, the  $45 \times 45$  matrix is diagonalized, and the program fits the calculated eigenvalues to those observed spectrally, by least-squares analysis. A "HUNT" subroutine is employed whereby each of the eight ligand field parameters (including  $B$ ,  $C$ , and  $\zeta$ ) is varied individually until the fit function is minimized. The results provide not only  $B$ ,  $C$ , and  $\zeta$ , the 45 eigenvalues, and the

(41) J. L. Prather, *Nat. Bur. Stand. (U. S.), Monogr. No. 19* (1961).

(42) M. T. Hutchings and W. P. Wolf, *J. Chem. Phys.*, **41**, 617 (1964).

(43) G. E. Shankle, Ph.D. Dissertation, University of Tennessee, 1968.

coefficients of the crystal field potential expansion in the low-symmetry field but also the percentage triplet-singlet character of each eigenvalue.

The energies of the best fit of the calculated levels are indicated in Figure 5. A  $Dq$  value of approximately  $1000 \text{ cm}^{-1}$  ( $Dq$  for bis(glycinato)bis(imidazole)nickel(II) complexes has been reported<sup>44</sup> as  $982 \text{ cm}^{-1}$ ) was used as an initial input parameter along with the estimated values of  $B = 937 \text{ cm}^{-1}$ ,  $C = 3750 \text{ cm}^{-1}$ , and  $\lambda = -280 \text{ cm}^{-1}$ . In perfect octahedral geometry the nonzero coefficients  $\Gamma_{40}$  and  $\Gamma_{44}$  are related by the fixed ratio  $(5/7)^{1/2}$ . In addition, in a tetragonal field  $\Gamma_{44}$  can be related to the crystal field parameter  $Dq$  by the relationship  $\Gamma_{44} = 2(35\pi)^{1/2}Dq$ . For the  $d^8$  configuration the  $\Gamma_{nm}$  coefficients are related to the  $\gamma_{nm}$  parameters used by Hutchings<sup>42</sup> in his expansion of the crystal field potential as in<sup>40,43</sup>

$$\Gamma_{nm}^c = -|e| \langle r^k \rangle \gamma_{nm}^c$$

where  $|e|$  is the electronic charge and  $\langle r^k \rangle$  is the  $k$ th power of the radial integral. The  $\Gamma_{nm}^c$  coefficients which give the best fit of the calculated levels to the observed levels are listed in Table III. The fit function

TABLE III  
LIGAND FIELD PARAMETERS AND ENERGY LEVELS  
CALCULATED FOR Ni(DL-his)<sub>2</sub>·H<sub>2</sub>O

Parameters, cm <sup>-1</sup>	Excited State	Energy, cm <sup>-1</sup>		
		Calcd <sup>b</sup>	Obsd	
$B = 783$	<sup>3</sup> T <sub>2g</sub> (F)	A <sub>1</sub>	10,658	10,600
$C = 3653$		B <sub>2</sub>	11,300	...
		A <sub>2</sub>	11,903	11,400
$\Gamma_{20} = 6238; B_0^2 = 3930^a$	<sup>1</sup> E <sub>g</sub>	A <sub>1</sub>	13,130	12,800
$\Gamma_{40} = 8458; B_0^4 = 7155$		B <sub>2</sub>	16,556	16,500
$\Gamma_{22} = -18.2; B_2^2 = -8.1$	<sup>3</sup> T <sub>1g</sub> (F)	B <sub>1</sub>	18,864	18,800
$\Gamma_{42} = -28,392; B_2^4 = -16,982$		A <sub>2</sub>	19,397	19,000
$\Gamma_{44} = -23,517; B_4^4 = -14,066$		A <sub>1</sub>	21,900	21,600 <sup>c</sup>
	<sup>3</sup> T <sub>1g</sub> (P)	B <sub>2</sub>	27,298	27,300
		B <sub>1</sub>	28,870	28,900
		A <sub>2</sub>	29,861	29,800

<sup>a</sup> See B. G. Wybourne, "Spectroscopic Properties of Rare Earths," Interscience, New York, N. Y., 1965, for a definition of the  $B_{nm}^k$  coefficients, which have been related to the  $\Gamma_{km}$ 's by Couch.<sup>40</sup> <sup>b</sup> Calculated with  $\zeta = +500$ . After  $\zeta$  was changed from +50 to +500, no iterations were done to refine the fit. <sup>c</sup> Not used in fitting procedure.

for this fit is  $5 \times 10^6$  for an average agreement of the nine levels fitted of  $\pm 100 \text{ cm}^{-1}$ . The comparison of the observed and calculated levels is given in Figure 5.

## Discussion

The purpose of this work and of similar studies<sup>45-55</sup> has been to gain an enhanced understanding of a molecular spectrum by using a single crystal as an orienting matrix in which to measure low-temperature and polar-

(44) G. N. Rao and N. C. Li, *Can. J. Chem.*, **44**, 1637 (1966).

(45) N. S. Hush and R. J. M. Hobbs, *Progr. Inorg. Chem.*, **10**, 259 (1968).

(46) R. L. Belford and J. W. Carmichael, Jr., *J. Chem. Phys.*, **46**, 4515 (1967).

(47) C. Simo, E. Banks, and S. L. Holt, *Inorg. Chem.*, **8**, 1446 (1969).

(48) B. J. Hathaway, M. J. Bew, D. E. Billing, R. J. Dudley, and P. Nicholls, *J. Chem. Soc. A*, 2312 (1969).

(49) S. L. Holt and C. Simo, *J. Inorg. Nucl. Chem.*, **32**, 457 (1970).

(50) C. Simo, E. Banks, and S. L. Holt, *Inorg. Chem.*, **9**, 183 (1970).

(51) B. J. Hathaway, R. J. Dudley, and R. J. Fereday, *J. Chem. Soc. A*, 571 (1970).

(52) L. Dubicki, M. A. Hitchman, and P. Day, *Inorg. Chem.*, **9**, 188 (1970).

(53) R. Dingle, *J. Chem. Phys.*, **50**, 545 (1969).

(54) E. M. Holt, S. L. Holt, and K. J. Watson, *J. Amer. Chem. Soc.*, **92**, 2721 (1970).

(55) R. Dingle, P. J. McCarthy, and C. J. Ballhausen, *J. Chem. Phys.*, **50**, 1957 (1969).

ized spectra. Although many of the above studies have concerned themselves with systems of relatively high symmetry, fewer studies have been carried out in which the metal ion environment differs greatly from the idealized purely octahedral symmetry. To be most successful in such an investigation one must be assured that the crystal spectra are essentially of molecular origin and not characterized by appreciable solid-state effects. That is, can we consider that the crystal acts like an oriented gas with respect to its interaction with electromagnetic radiation? If this is so, we should find that the solution spectra are reproduced in terms of band maxima, shapes, and areas by a statistical summation of the distinct crystal spectra. In the case of the orthorhombic crystals of  $\text{Ni}(\text{DL-his})_2 \cdot \text{H}_2\text{O}$  the requisite equation is

$$\epsilon_{\text{soln}} = 1/3(\epsilon_a + \epsilon_b + \epsilon_c)$$

where  $\epsilon_a$ ,  $\epsilon_b$ , and  $\epsilon_c$  are the molar absorptivities measured along the crystallographic axes at 300°K. When plotted, this summation agrees reasonably well with the spectrum of the pH 10 solution from which the crystals were grown. Band maxima and shapes are very closely in agreement. Therefore, we conclude that the oriented gas approximation is valid, at least for explaining the electronic spectrum. The small differences in band shapes and intensities are likely caused by the effects of lattice vibrations on the crystal spectrum.

The determination of the spectra polarized along the molecular axes as opposed to the spectra polarized along the extinction directions in the crystal ( $a$ ,  $b$ , and  $c$ ) has been made by the relationships

$$\begin{aligned} \epsilon_z &= \epsilon_c \\ \epsilon_y &= \frac{\epsilon_a \cos^2 \theta - \epsilon_b \sin^2 \theta}{\cos^4 \theta - \sin^4 \theta} \\ \epsilon_x &= \frac{\epsilon_a \sin^2 \theta - \epsilon_b \cos^2 \theta}{\sin^4 \theta - \cos^4 \theta} \\ \theta &\simeq 11^\circ \end{aligned}$$

These are essentially the same relationships as those used by Piper and Carlin<sup>56,57</sup> and by others.<sup>58</sup> As pointed out by Belford,<sup>59</sup> they are based on the approximation that, for light polarized along an extinction direction ( $a$ ,  $b$ , or  $c$ ), the probabilities of interaction with the electric dipole components of the molecules are proportional to the products of the squares of the electric vector projections on the molecular axes and the intrinsic molecular absorptivities ( $\epsilon_x$ ,  $\epsilon_y$ , and  $\epsilon_z$ ). The interesting result of this calculation is that considerable lack of orientation of the molecular axes with the directions of polarization of light is allowed before there is an appreciable deterioration of the polarization ratio, even when the polarization ratio is relatively large. For example, although the shoulder at 27.3 kK in the  $b$  spectrum of the racemic crystal (Figure 2) is apparently due to the fraction of  $y$  molecular polarization contained, the bands at 16.5 and 19.0 kK in the  $b$  spectrum cannot be ascribed to nonorientation, since they

(56) T. S. Piper, *J. Chem. Phys.*, **35**, 1240 (1961).

(57) T. S. Piper and R. L. Carlin, *Inorg. Chem.*, **2**, 260 (1963).

(58) See for example J. Ferguson, *J. Chem. Phys.*, **32**, 533 (1960); **34**, 1609 (1961); F. A. Cotton and J. J. Wise, *Inorg. Chem.*, **6**, 917 (1967); R. Dingle, *Acta Chem. Scand.*, **22**, 2219 (1968).

(59) T. S. Piper, *J. Chem. Phys.*, **36**, 1089 (1962). Our discussions with Professor Belford are also acknowledged.

are only slightly diminished by the correction. Similar behavior had been mentioned by Burns in his polarized studies of crystals of fayalite,  $\text{Fe}_2\text{SiO}_4$ .<sup>60</sup>

The discussion which follows will be concerned only with the racemic crystal  $\text{Ni}(\text{DL-his})_2 \cdot \text{H}_2\text{O}$ , since the most accurate data were obtained on samples of this system. As mentioned earlier, spectra of  $\text{Ni}(\text{L-his})_2 \cdot \text{H}_2\text{O}$  served as a comparison with the DL case in order to justify the assumption that the spectra interpreted are essentially molecular spectra and to demonstrate another example of spectra obtained from Ni(II) in a low-symmetry site.

The effective electronic symmetry of the racemic complex is obviously a distortion of octahedral symmetry, since the three ligand field bands characteristic of octahedral nickel(II) are clearly observed. The unusually large number of band maxima, the very strong polarizations of individual maxima, and the generally small temperature dependence of the intensities suggest that the intensity-gaining mechanism most important in weakening the Laporte selection rule ( $g \leftrightarrow g$ ) is the low symmetry of the effective field around the metal atom. The low symmetry of the ligand field not only results from the electronic differences in the donor atoms but, as shown in the crystal structure,<sup>31</sup> is also to be associated with the considerable distortion of the coordination sphere from regular octahedral geometry.

We note first that the site symmetry of the nickel and the molecular symmetry of the compound are  $C_2$ . The spectra, however, do not obey  $C_2$  selection rules. If they did, all maxima which appear in  $x$  should also appear in  $y$ . Figure 3 illustrates that this is not so. The symmetry of the coordination sphere, that is, of the metal atom plus the six donor atoms, is  $C_{2v}$ . The spectra obviously indicate that the  $x$ ,  $y$ , and  $z$  molecular axes are electronically distinct (which is the case in the triaxial point group  $C_{2v}$ ). The lack of significant overall temperature dependence indicates that the spectral band intensity is due mainly to a static crystal field and confirms the absence of a center of symmetry in the electronic structure as well as the molecular structure. From these considerations we conclude that the most likely point group in which to assign the spectra is  $C_{2v}$ .  $D_2$ , although isomorphous with  $C_{2v}$ , is rejected because of the pronounced difference between the O-Ni-O and O-Ni-N<sub>A</sub> angles (100.3° vs. 79.7°), as well as the inequivalence of the O and N<sub>A</sub> donors. The related higher symmetry groups  $D_{2h}$ ,  $C_{2h}$ , and  $D_{4h}$  require a center of symmetry and, for  $C_{2h}$  and  $D_{4h}$  equivalence of the  $x$  and  $y$  molecular axes.

Tetragonal complexes of nickel(II) have received considerable attention.<sup>61-66</sup> Rowley and Drago<sup>61,62</sup> obtained spectra showing six band maxima indicating splitting of each <sup>3</sup>T level into a singly and doubly degenerate (orbital) level. The tetragonal distortion of complexes of the type  $\text{Ni}(\text{amine})_4(\text{ClO}_4)_2$ , with substituted anilines, in which the lowest energy, spin-

(60) R. G. Burns, *J. Sci. Instrum.*, **43**, 58 (1966).

(61) D. A. Rowley and R. S. Drago, *Inorg. Chem.*, **7**, 795 (1968).

(62) D. A. Rowley and R. S. Drago, *ibid.*, **6**, 1092 (1967).

(63) A. V. Butler, D. J. Phillips, and J. P. Redfern, *J. Chem. Soc. A*, 1064 (1968).

(64) D. M. L. Goodgame, M. Goodgame, M. A. Hitchman, and M. J. Weeks, *ibid.*, **A**, 1769 (1968).

(65) G. Maki, *J. Chem. Phys.*, **29**, 162, 1129 (1958).

(66) G. Maki, *ibid.*, **28**, 651 (1958).

allowed  ${}^3T_{2g}$  band is split by approximately 3000  $\text{cm}^{-1}$ , has been discussed.<sup>63</sup> Other spectral studies of tetragonally distorted nickel(II) complexes include investigations of complexes of the type  $\text{NiL}_4\text{X}_2$  (where L = heterocyclic amine ligands and X = Br, Cl, or I).<sup>64</sup> Maki has discussed the ligand field theory of nickel(II) complexes in various low-symmetry point groups<sup>65</sup> and has assigned the solution spectrum of  $\text{Ni}(\text{gly})_2 \cdot 2\text{H}_2\text{O}$  in  $D_{2h}$  symmetry.<sup>66</sup> Rao and Li, however, interpreted spectra of complexes such as bis(amino acid)bis(imidazole)nickel(II) in terms of  $O_h$  symmetry.<sup>44</sup>

In order to assign the molecular axes and relate the octahedral energy levels to those arising in  $C_{2v}$ , the following correlation is carried out. The molecular and site symmetries place the  $C_2(z)$  axis of the  $C_{2v}$  point group along the bisector of the  $\text{N}_A\text{-Ni-N}_A$  and  $\text{O-Ni-O}$  angles. The  $\sigma_h$  plane in the parent  $O_h$  group becomes the  $\sigma_v(xz)$  plane in  $C_{2v}$ ; the remaining  $\sigma_v(yz)$  plane of the lower symmetry group then correlates with a  $\sigma_d$  plane of  $O_h$ . The complete correlation as it effects the electronic energy levels present is shown in Table IV. (A convenient correlation as employed by Wilson,

TABLE IV  
CORRELATION OF  $O_h$  WITH  $C_{2v}$

$O_h$	$E$	$C_2$	$\sigma_h$	$\sigma_d$	
	$E$	$C_2$	$\sigma_v(xz)$	$\sigma_v(yz)$	$C_{2v}$
$A_{2g}$	1	-1	1	-1	$B_1$
$T_{2g}$	3	1	-1	1	$A_1 + A_2 + B_2$
$T_{1g}$	3	-1	-1	-1	$A_2 + B_1 + B_2$

Decius, and Cross<sup>67</sup> leads to the same results if the correlation is carried out through the  $D_{4h}$  point group (see Figure 5). In that case, the  $z$  axis in  $C_{2v}$  is a former  $C_2''$  axis in  $D_{4h}$ , where the  $\text{N}_I\text{-Ni-N}_I$  direction is assumed to be coincident with the  $z$  axis of  $D_{4h}$ . The strong dichroism of the crystals suggests that the  $\text{N}_I\text{-Ni-N}_I$  direction is very "different" from the other two directions. Thus, the complex *could* be considered tetragonal in nature as illustrated in the correlation diagram of Figure 5. The geometry of the complex would then suggest a small "axial" ( $D_{4h}$ ) perturbation (all bond lengths are about 2.10 Å), but a large "in-plane" rhombic distortion. The relation of this choice of symmetry axes to the geometry of the molecule is seen in Figure 1.

The ground state of the complex will have  ${}^3B_1$  symmetry. In  $C_{2v}$  the electric dipole operators  $\mu_x$ ,  $\mu_y$ , and  $\mu_z$  transform as  $B_1$ ,  $B_2$ , and  $A_1$ , respectively. Assuming a purely electric dipole mechanism, the selection rules for the various possible  ${}^3B_1 \rightarrow \Gamma_{es}$  transitions are summarized as follows for light polarized along the  $x$ ,  $y$ , and  $z$  molecular axes ( $\times$ , forbidden;  $\checkmark$ , allowed).

$\mu$	$\Gamma_{es}$			
	$A_1$	$A_2$	$B_1$	$B_2$
$x$	$\checkmark$	$\times$	$\times$	$\times$
$y$	$\times$	$\checkmark$	$\times$	$\times$
$z$	$\times$	$\times$	$\checkmark$	$\times$

The molecular spectra in Figure 3 only approximately correlate with the selection rules above. The best agreement is in the infrared band system where intensity is only predicted in the  $x$  and  $y$  polarizations. The  $z$  spectrum shows less than 20% of the intensity of the  $x, y$  average. In the two band systems arising from the

octahedral levels  $T_{1g}(F)$  and  $T_{1g}(P)$ , intensity is predicted in only the  $y$  and  $z$  polarizations and in each case in only a single transition. Actually, two bands are observed in the  $y$  polarizations of both the  $T_{1g}(F)$  and  $T_{1g}(P)$  systems and in the  $x$  polarization of the  $T_{1g}(F)$  system. In these multiplets a single  $z$ -polarized band appears. In summary, we see twelve bands as listed in Table I and illustrated in Figure 5: six which correlate with the electric dipole selection rules and six which do not. A shoulder on the high-energy side of the lowest energy transitions at 12.8 kK can be attributed to the spin-forbidden  ${}^1E$  band. A weak band also occurs at 21.6 kK in the  $z$  polarization, but *not* in the  $x$  and  $y$  polarizations. Although this is in the region often attributed to the spin-forbidden  ${}^1A_1$  transition, the polarization of the band suggests that it may be due to an overtone of the water  $\text{OH}^-$  stretching frequency superimposed on the electronic transition at 19.0 kK. Because of this ambiguity this band was not included in the fitting procedure.

The most likely explanation for the appearance of the electronically "forbidden" bands is vibronic coupling. If this is the case, we might expect that the temperature dependence of the "forbidden" bands would be markedly greater than that of the allowed bands. From the data in Table I we see that this is indeed so. For most bands the range of per cent temperature decrease for those assigned as allowed transitions is 5-10% and for the forbidden bands is 30-55%. The vibrational modes of the  $C_{2v}$  coordination sphere and metal ion are 6  $\alpha_1$ , 2  $\alpha_2$ , 4  $\beta_1$ , and 3  $\beta_2$ . The symmetries of the modes required to induce intensity in each of the "forbidden" spin-allowed transitions are given in Table I along with an estimate of its energy as calculated by the approximation of Holmes and McClure.<sup>37</sup>

Bosnich<sup>68</sup> has used one-electron d orbitals for square-planar nickel(II) salicylaldehyde complexes in  $C_{2v}$  symmetry. Using projection operators we have obtained similar orbitals as illustrated in Table V.

TABLE V  
SYMMETRY OF ORBITALS IN  $C_{2v}$  ( $C_2''$ )

Symmetry	Orbital	Symmetry	Orbital
$b_1$	$x^2 - y^2$		
$a_1$	$z^2$	$b_2$	$\frac{1}{\sqrt{2}}(xz + yz)$
$a_1$	$xy$	$a_2$	$\frac{1}{\sqrt{2}}(yz - xz)$

Using a coordinate system similar to that described in Figure 7a of ref 68 (where the  $\text{N}_I\text{-Ni-N}_I$  direction is  $z(y')$  and the  $x'$  axis bisects the amino acid rings) the following energy ordering is suggested by the physical model

$$z^2 > x^2 - y^2 > xy > \frac{1}{\sqrt{2}}(xz - yz) > \frac{1}{\sqrt{2}}(xz + yz)$$

This assignment yields energy levels which agree with the calculated order of levels arising from the lowest ( ${}^3T_{2g}(F)$ ) band system. The order predicted by this elementary model for the  ${}^3T_{1g}(F)$  band system ( $B_1 < A_2 < B_2$ ), however, does not agree with that calculated by DWOSCH or observed spectroscopically.

The assignments verify that the "in-plane" distortion of ca.  $10^\circ$  is more significant than the "tetragonal"

(67) E. B. Wilson, Jr., J. C. Decius, and P. C. Cross, "Molecular Vibrations," McGraw-Hill, New York, N. Y., 1955.

(68) B. Bosnich, *J. Amer. Chem. Soc.*, **90**, 627 (1968).

distortion along the  $N_I$ -Ni- $N_I$  axis. (Similar distortions have also been observed in single crystals of glycine complexes with nickel(II).<sup>69</sup> This lends spectral support to earlier chemical studies which have shown that the bond between a secondary or tertiary nitrogen atom and a metal atom is weaker than that between a primary nitrogen and the same metal ion.<sup>7</sup> Reflectance spectra of complexes of the type  $Ni(\text{imidazole})_6X_2$  (where  $X^- = Cl^-, Br^-, I^-,$  or  $NO_3^-$ ) have produced<sup>70</sup>  $Dq$  values  $\approx 1050\text{ cm}^{-1}$ , whereas Jørgensen observed<sup>39</sup> an  $Ni(\text{gly})_3^-$  complex with  $Dq = 1010\text{ cm}^{-1}$ , while an  $Ni(\alpha\text{-ala})_3^-$  anion has been reported<sup>71</sup> with  $Dq = 995\text{ cm}^{-1}$ . Thus, for the ligands involved, the spectroscopic effect of the tetragonal distortion along the  $N_I$ -Ni- $N_I$  is expected to be small. The assignments above confirm that the "in-plane" distortion is most effective in determining the observed energy levels.

The assignments of the energy levels based on spectroscopic polarization studies have been verified by the ligand field calculations using DTWOSCH. Nine experimentally determined levels were fit (by least-squares analysis) to within an average of  $\pm 100\text{ cm}^{-1}$  of the calculated eigenvalues. Only one level was calculated in a position significantly different from the observed levels. This was the  ${}^3B_2$  level arising in the  ${}^3T_{2g}(O_h)$  multiplet. Predicted to be forbidden by electric dipole selection rules, it is calculated to lie at 11.3 kK. It appears, therefore, that the weak band observed in the  $z$  polarization at 10.5 kK and tentatively assigned to vibronic intensity in the  ${}^3B_2$  band is really associated with vibronic intensity in the  ${}^3A_1$  level and that the  ${}^3B_1$  level is not observed. This means that the splitting of the  ${}^3E(D_{4h})$  component by the rhombic distortion is smallest in the lowest multiplet (a circumstance observed in a previous calculation<sup>40</sup>).

Because of the uncertainty of assignment of the weak band at 21.6 kK the  ${}^1A_1$  level was not included in the fit. However, based on the fit of the other levels the  ${}^1A_1$  band is calculated to be at 21.9 kK. This tends to support the assignment of the 21.6-kK band to this transition although planned spectra of deuterated crystals should effectively settle this point.

Using this fit the following ligand field parameters were estimated:  $Dq = -1125\text{ cm}^{-1}$ ,  $B = 783\text{ cm}^{-1}$ , and  $C = 3653\text{ cm}^{-1}$ . Since no experimental evidence for spin-orbit splitting was available, a value of  $\zeta = -500$  (which is reduced from the free-ion value by approximately the same amount as  $B$  and  $C$ ) was used in the final fit.

### Conclusion

Most previous reports of the polarized spectra of single crystals have involved high-symmetry crystals

and chromophores of uniaxial symmetry with their symmetry axes aligned. However, a few studies have been reported in which one or more of these conditions did not obtain. We have shown in this report that reasonably accurate molecular spectra may be obtained by relatively simple handling of the spectra of biaxial crystals containing nonaligned, triaxial chromophores. The implication is that useful, detailed crystal spectra may be obtained in cases previously shunned or only cursorily analyzed because of low symmetry.

It is also obvious that the electronic spectra of amino acid complexes, often only studied in solution and interpreted in terms of high-symmetry ligand fields,<sup>44</sup> can provide valuable information about the environment of the metal atom (even when the donor atoms are very similar) if studied in the solid state at cryogenic temperatures. Similar studies of more complicated species of biological importance, *e.g.*, metalloenzymes, in oriented single crystals should allow the metal atom to serve as a sensitive "probe" near the active site.<sup>72,73</sup>

Williams, *et al.*,<sup>72,73</sup> have discussed in detail the advantages of studying the properties of enzymes in which the metal atom can serve as an electronic marker. They also make two important observations which are perhaps pertinent to the results reported here: (1) that metals (*e.g.*, cobalt(II) and zinc(II)) which show catalytic power, in contrast to many other metals, often enter sites of low symmetry readily, which appear to be of special catalytic potential and (2) that where a metalloenzyme is active, detailed analysis of the spectroscopic properties show that the geometry of the metal-binding site is low symmetry.

Extension of studies similar to the one reported here to single crystals of metal-activated enzymes substituted with metal atoms whose electronic structure is relatively well-known, as is the case for  $d^8$  nickel(II) (even though nickel(II) may not activate the enzyme very well), may provide valuable information about the low-symmetry environment of the active sites in which protein residues (*e.g.*, the imidazole of histidine) coordinate to the metal in less than idealized symmetry. As in this simple "model" compound, these studies might allow a more detailed interpretation of the nature, symmetry, and orientation of the metal-binding site.

**Acknowledgment.**—This research has been supported by grants from the Duke University Biomedical Sciences Support Grant and the Duke University Computation Center and by fellowships to P. L. M. from the Shell Oil Co. The authors wish to thank Dr. M. M. Harding for the availability of crystallographic results prior to publication. The generous provision of the program DTWOSCH and considerable consultation on its application by Dr. T. W. Couch are also gratefully acknowledged as are many helpful discussions of the theory with Mr. Paul Wormer.

(69) H. C. Freeman, J. M. Guss, and R. L. Sinclair, *Chem. Commun.*, 485 (1968).

(70) W. J. Eilbeck, F. Holmes, and A. E. Underhill, *J. Chem. Soc. A*, 757 (1967).

(71) V. S. Sharma, H. B. Mathur, and A. B. Biswas, *Indian J. Chem.*, **2**, 5 (1964).

(72) B. L. Vallee and R. J. P. Williams, *Chem. Brit.*, **4**, 397 (1968).

(73) A. E. Dennard and R. J. P. Williams, *Transition Metal Chem.*, **2**, 115 (1966).